Available online at www.sciencedirect.com
SCIENCE DIRECT
Polymer 46 (2005) 243–252
polymer
www.elsevier.com/locate/polymer

Strengthening acrylonitrile-butadiene-styrene (ABS) with nano-sized and micron-sized calcium carbonate

L. Jiang[a], Y.C. Lam[a,*], K.C. Tam[a], T.H. Chua[a], G.W. Sim[b], L.S. Ang[b]

[a]*School of Mechanical and Production Engineering, Nanyang Technological University, 50 Nanyang Avenue, Singapore 639798, Singapore*
[b]*NanoMaterials Technology Pte Ltd, 26, Ayer Rajah Crescent #07-02, Singapore 139944, Singapore*

Received 21 June 2004; received in revised form 27 October 2004; accepted 1 November 2004
Available online 21 November 2004

Abstract

ABS was reinforced by both micron-sized (MCC) and nano-sized precipitated calcium carbonate (NPCC) particles through melt compounding. The MCC/ABS composites were found to have higher modulus but lower tensile and impact strength than neat ABS. In contrast, NPCC increased modulus of ABS whilst maintained or even increased its impact strength for a certain NPCC loading range. SEM examinations revealed that NPCC particles/agglomerates were distributed in much smaller sizes in the composites than its MCC counterparts. The larger interfacial area between NPCC and ABS and cavitation-induced shear yielding in the ligament are believed to be the main reasons of the mechanical property improvement of the NPCC/ABS composites. NPCC/ABS also shows completely different rheological behavior from MCC/ABS, such as the loss of Newtonian region, high G' at low frequencies and the appearance of yield phenomenon. A NPCC network structure was believed to be formed in the composites and induced these pseudo-solid-like rheological behaviors.

Keywords: ABS; Calcium carbonate; Nanocomposites

1. Introduction

Inorganic particulate fillers have been employed to improve properties and/or lower costs of polymer products effectively. Young's modulus, hardness, heat distortion temperature, thermal expansion (mould shrinkage) etc. of the filled polymers could be improved to various extents. In general, nano-sized fillers are superior to their micron-sized counterparts in improving mechanical and thermal properties of thermoplastics due to the larger interfacial area between the particles and the surrounding polymer matrix [1–6]. Nano-sized fillers could increase modulus and hardness of some polymers but still maintain or even increase their tensile and/or impact strength in a certain filler loading range [7–14]. Nano-sized fillers are also preferred when transparency, surface smoothness, fire retardancy and barrier property of the composites are the priorities.

Polymer/layered-silicate nanocomposites have been most extensively studied possibly due to the natural abundance of silicate clay. Organic/inorganic hybrid structure is formed when polymer chains are placed into the silicate interlayers or galleries. The structure is intercalated if a single, extended polymer chain is intercalated between the host layers, resulting in a well ordered multilayer with alternating polymer/inorganic layers and a repeat distance of a few nanometers. When the silicate layers are completely and uniformly dispersed in a continuous polymer matrix, an exfoliated or delaminated structure is obtained. If the polymer is unable to intercalate between the silicate layers, a phase separated composite is obtained, whose properties may stay in the same range as the traditional microcomposites when the lateral dimensions of the silicate are large. To synthesize the intercalated or exfoliated hybrid structure, different routes such as in situ polymerization, solution blending, melt compounding, or template synthesis can be used [15]. Among them, melt compounding employs currently available techniques such

* Corresponding author. Tel.: +65 6790 5866; fax: +65 6791 1859.
E-mail address: myclam@ntu.edu.sg (Y.C. Lam).

0032-3861/$ - see front matter © 2004 Elsevier Ltd. All rights reserved.
doi:10.1016/j.polymer.2004.11.001

as extrusion and chamber mixing, and is broadly applicable to a range of commodity polymers. Thus it has the lowest barrier to mass production.

Micron-sized calcium carbonate is historically used to lower the cost of relatively expensive polymer resins. It has very limited effects on property improvement due to the poor particle–polymer interaction. Efforts have been made to modify the surface of $CaCO_3$ particles so as to increase the interaction [16,17]. Calcium carbonate does not have a layered structure and therefore there is no intercalation or exfoliation in nano-sized $CaCO_3$/polymer composites. However, due to the larger interfacial area in nano-sized $CaCO_3$/polymer, its properties are expected to be better than the micron-sized $CaCO_3$/polymer composites. Nano-sized $CaCO_3$ was found to increase the glass transition and melting temperature of poly(ethylene terephthalate) (PET) and also act as a neucleating agent [18]. Nanoparticles of $CaCO_3$ also significantly increased tensile modulus and impact strength of polypropylene/$CaCO_3$ nanocomposites while maintained their ultimate and yield stress and strain [19]. However, poly(propylene carbonate) (PPC)/$CaCO_3$ nanocomposites were also found to be inferior to their micron-sized counterparts in mechanical properties due to the poor dispersion of the nanoparticles [20].

ABS/$CaCO_3$ composites received very limited research interests. Liang et al. studied some rheological properties of the composites such as shear viscosity, extension viscosity, and entry pressure drop by capillary extrusion [21,22]. Mechanical property study revealed increase in tensile modulus but decrease in tensile and impact strengths. Particle size and surface treatment were found to have insignificant effect on the properties [23].

In this investigation, micron-sized and nano-sized calcium carbonate/ABS composites were studied. Particle dispersion and mechanical properties were compared. In addition, rheological measurements were employed to study their microstructures in the melt state.

2. Experimental

2.1. Materials

Toyolac 700 ABS, a copolymer of acrylonitrile (23%), butadiene (13%) and styrene (64%) was obtained from Toray Industries (Japan). This general purpose grade ABS has a molecular weight (M_w) of 13,000 and a melt flow index (ISO-1133) of 23 g/10 min at 220 °C.

The nano-sized precipitated calcium carbonate is NPCC-201 from NanoMaterials Technology (Singapore). It was coated with stearic acid to increase dispersion and compatibility with the polymer matrix. The calcium carbonate particulates are in cubic shape with an average primary particle size of ~40 nm. It was designed to be a reinforcing additive to improve the various properties of plastic materials. The micron-sized calcium carbonate (MCC) is from Omya AG. It has a mean particle size of ~5 μm and is commonly used in the polymer industry to increase modulus and/or lower costs. The powder was also stearic acid coated for better dispersion.

2.2. Sample preparation and testing

A Haake Conical Twin Screw Extruder (Rheomex TW100) was employed to disperse NPCC and MCC into ABS homogeneously. Before extrusion, ABS, NPCC and MCC were dried in a vacuum oven at 60 °C for 24 h to remove absorbed moisture. The fillers were first pre-mixed with ABS manually in a zip-lock bag, and then poured into the hopper of the extruder. The extrusion temperature was 170 °C and the extrusion speed was 50 rpm. The extrudates were cooled down by a water bath before being granulated by a pelletizer. NPCC/ABS and MCC/ABS composites with 2, 4, 6, 8, 10, 20 and 30 wt% fillers were extruded. 0.2 wt% of antioxidant (Ciba IRGANOX 245) was added to each composite. The composites were vacuum dried and extruded the second time to achieve better filler dispersion. The extruder was purged thoroughly to remove contaminations each time before a new composite was extruded.

Standard tensile (ASTM D638) and Izod impact (ASTM D256) test samples were prepared by a Manumold 77/30 injection molding machine from Northampton Machinery Company (NMC). The composites were vacuum dried before injection molding. Barrel temperature was 190 °C. Tensile test was performed on an Instron 5569 with a crosshead speed of 10 mm/min. Izod impact test was performed using a Dynatup POE2000 impact test machine. All tests were carried out according to the ASTM standard and repeated four times for each sample to get an average value.

Filler distributions in the NPCC/ABS and MCC/ABS composites were studied by a JEOL 5600lv scanning electron microscope. The fractured surfaces from Izod impact test were observed. Pure NPCC and MCC powders were also examined by SEM. The filler particles were dissipated and de-agglomerated in ethanol by ultrasonic vibration. The suspensions were then dripped on a conductive carbon tape for SEM observation. Energy Dispersive X-ray Spectroscopy (EDXS) was also employed to detect the distribution of calcium atoms in NPCC/ABS composites.

Rheology study was conducted using a Rheometric Scientific ARES strain-controlled rheometer. Samples were tested on a parallel plate geometry measuring 25 mm in diameter at 200 °C. Strain sweep test was first carried out to determine the linear region of the materials. Then dynamic frequency sweep test was performed to determine the dynamic properties of the composites. Steady shear test was also conducted to investigate viscosity-shear rate relationship.

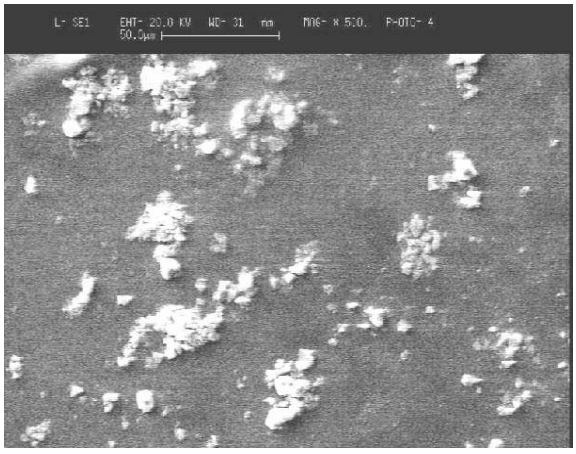

(a) MCC particles

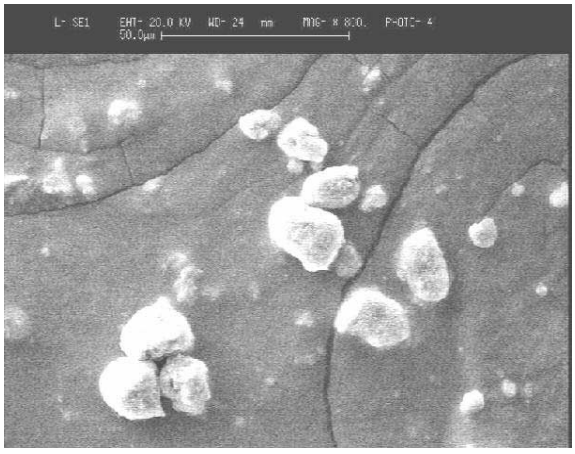

(b) NPCC particle agglomerations

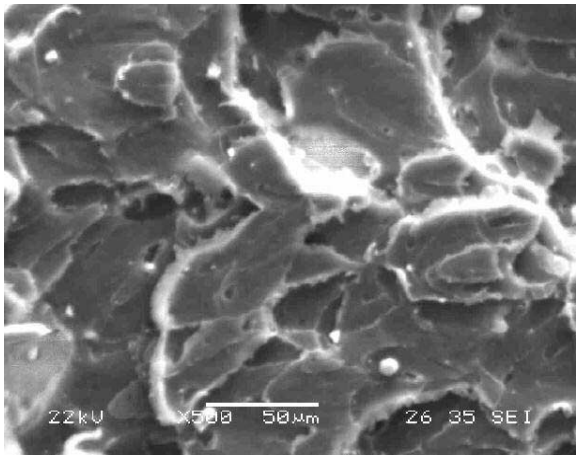

(c) 2% MCC/ABS

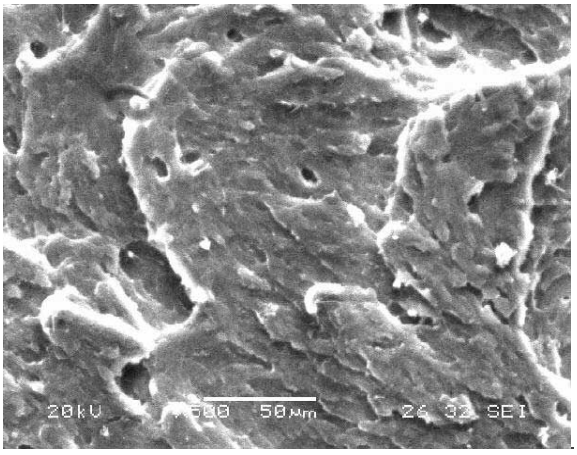

(d) 2% NPCC/ABS

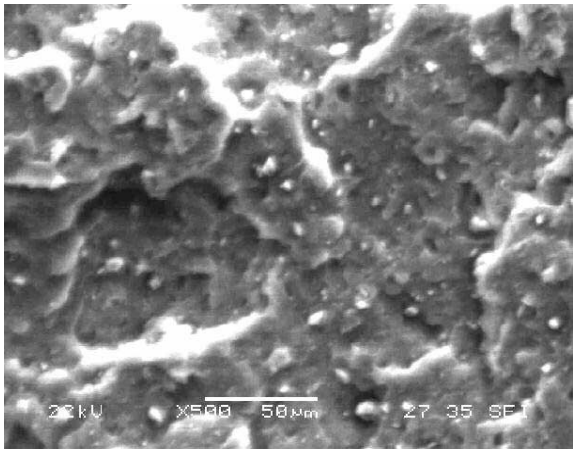

(e) 6% MCC/ABS

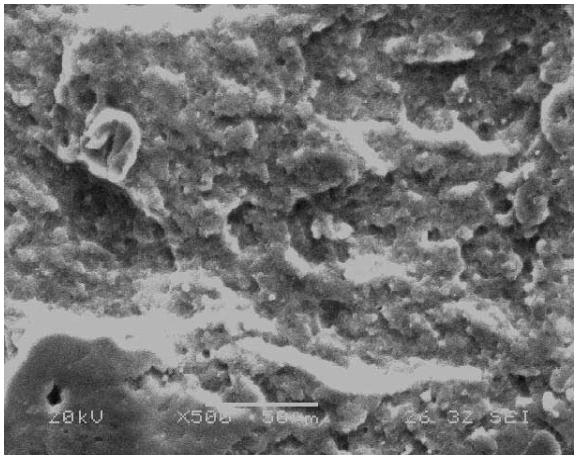

(f) 6% NPCC/ABS

Fig. 1. SEM micrographs of MCC/ABS and NPCC/ABS composites.

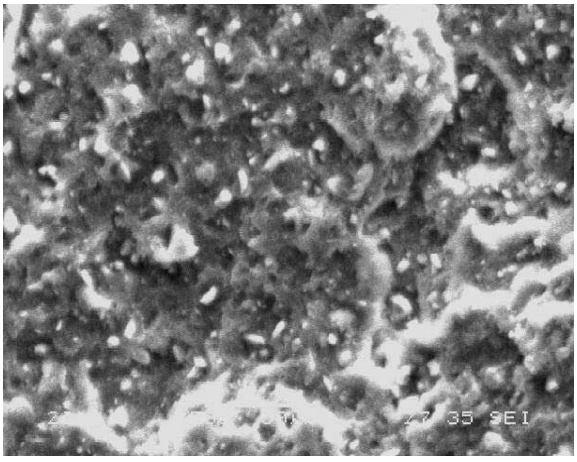

(g) 20% MCC/ABS

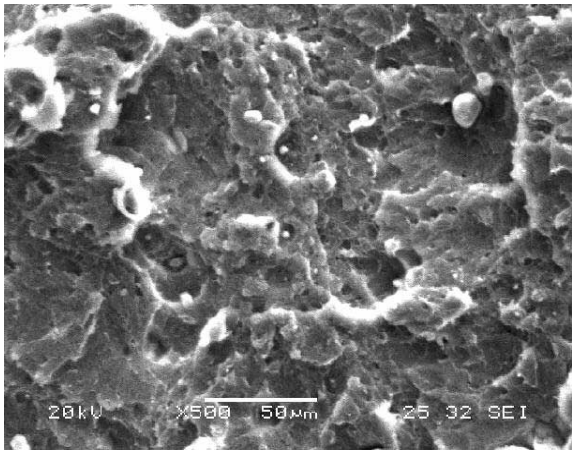

(h) 20% NPCC/ABS

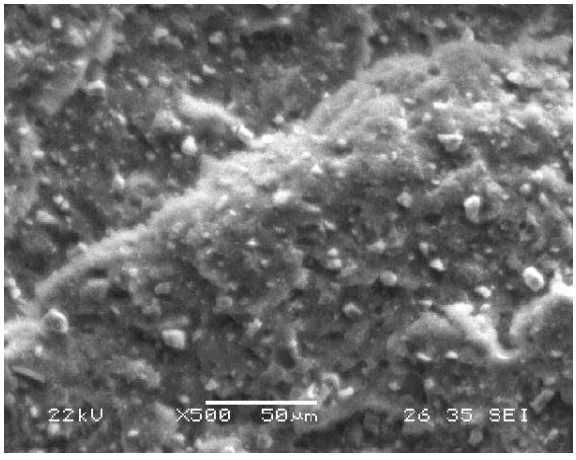

(i) 30% MCC/ABS

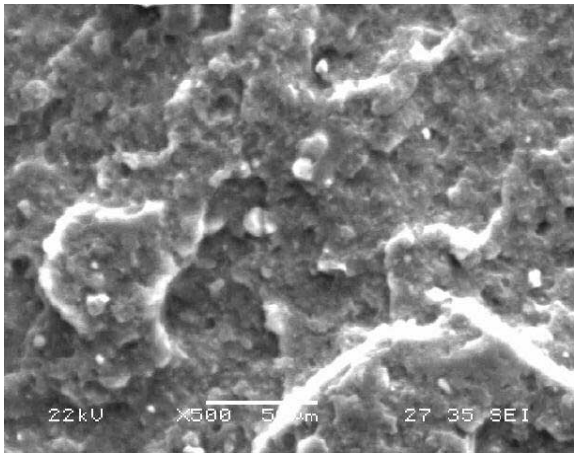

(j) 30% NPCC/ABS

Fig. 1 (*continued*)

3. Results and discussion

3.1. Dispersion of calcium carbonate particle

MCC and NPCC particles and their dispersions in the composites at different ratios are compared in Fig. 1(a)–(j). NPCC particles agglomerate due to their high surface tension. Even though ultrasonic vibration can de-agglomerate NPCC aggregates, they might quickly re-agglomerate after being dripped on the carbon tape. Fig. 1(b) shows a few

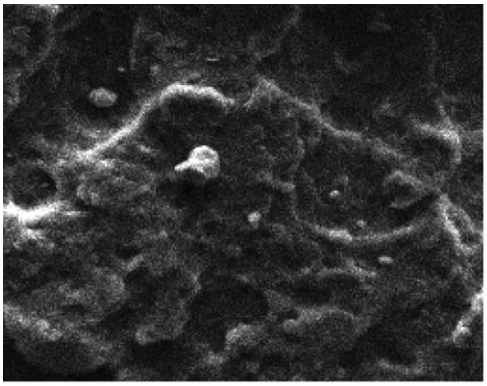

(a) SEM photo

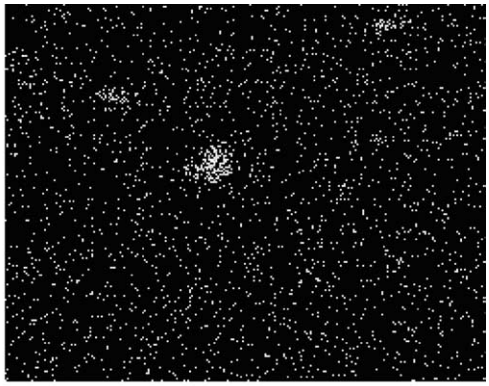

(b) EDXS mapping of calcium

Fig. 2. SEM and EDXS element mapping picture of NPCC/ABS.

NPCC agglomerates measuring as big as 20 μm. Agglomerates/particles with various sizes were present, where the nano-sized particles were too small to be observed. MCC was much easier to dissipate and they were mostly in single particles on the carbon tape, see Fig. 1(a).

The morphologies of MCC/ABS and NPCC/ABS composites were very different. In Fig. 1(c)–(j), the round white dots are powder particles/agglomerates. From these pictures only a few NPCC agglomerates can be observed at high filler ratios, whereas a large amount of MCC particles/agglomerates are observable even at low filler loadings. It is difficult to distribute nano-sized particles homogeneously into polymer matrix without agglomeration by melt compounding. However, these SEM micrographs show that the average particle/agglomerate size in NPCC composites was still much smaller than that in MCC composites.

Although NPCC is hardly observable in the SEM pictures, EDXS element mapping can verify its extensive distribution in the composites. Only a few NPCC agglomerates can be seen on the SEM picture in Fig. 2(a), but large amount of small white dots on the mapping picture reveal the traces of calcium atoms (Fig. 2(b)). This picture shows that although some NPCC particles existed in agglomerates as indicated by the dense-packed spots near the center of the mapping picture, most of the particles were evenly scattered throughout the matrix.

3.2. Mechanical

Micron-sized inorganic fillers have long been used in polymer industry to increase modulus and/or lower costs of the products. As expected, the moduli of MCC/ABS and NPCC/ABS composites increased with increasing filler contents as shown in Fig. 3. Fig. 3 indicates that MCC has a better modulus enhancing effect than NPCC. From literature, polymer layered silicate (PLS) nanocomposites are one of the most studied nanocomposites. Layered silicate exfoliates during the preparation of the composites and the exfoliated layers homogeneously disperse throughout the polymer matrix. In general, layered silicates have layer thickness on the order of 1 nm and a very high aspect ratio (e.g. 10–1000). A few weight percent of exfoliated layers thus have much larger interfacial area as compared to conventional composites. With strong polymer/filler interfacial action, tensile modulus of the composites increases drastically (a few times) at this low filler contents. The aspect ratio of the silicate layer and the extent of exfoliation strongly influence the final modulus of the composites, with higher aspect ratio and exfoliation extent leading to a larger modulus. The dispersion homogeneity of the exfoliated layers also plays an important role in property enhancement. In this research, NPCC was in cubic shape and there was no strong polymer/NPCC interaction at the interface. Therefore the reinforcing effect of NPCC was much less than that reported in the literature [24]. Indeed, the moduli of NPCC/ABS were even lower compared to MCC/ABS composites at the same filler content. Firstly, this could be due to more uneven dispersion of NPCC than MCC in ABS matrix as revealed by SEM micrographs. Secondly, modulus was calculated in the linear elastic region of the composites where the strain was less than 1.5%. Within this small strain, the stress was not high enough to break the bonding between the particles and ABS matrix. Therefore the larger interfacial area of NPCC/ABS did not contribute to modulus enhancement at this stage. On the other hand, the large size MCC particulates might be more effective in impeding the deformation of the polymer chain than small NPCC, and hence leaded to higher moduli of MCC/ABS composites.

In general, the modulus increased by inorganic fillers is achieved at the expense of tensile and impact strength, due to the filler-polymer interfacial weakness. As shown in Figs. 4 and 5, ultimate tensile strength and impact strength of MCC/ABS decreased with higher filler contents. Although the tensile strength of NPCC/ABS also decreased, the rate of decrease is less. At the same filler contents, NPCC/ABS had

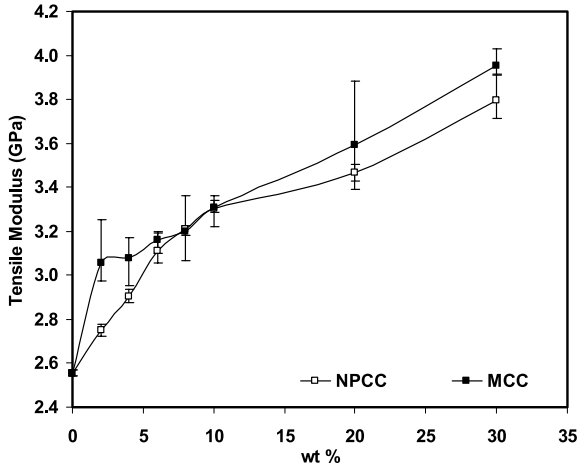

Fig. 3. Tensile moduli of NPCC/ABS and MCC/ABS composites with different powder contents.

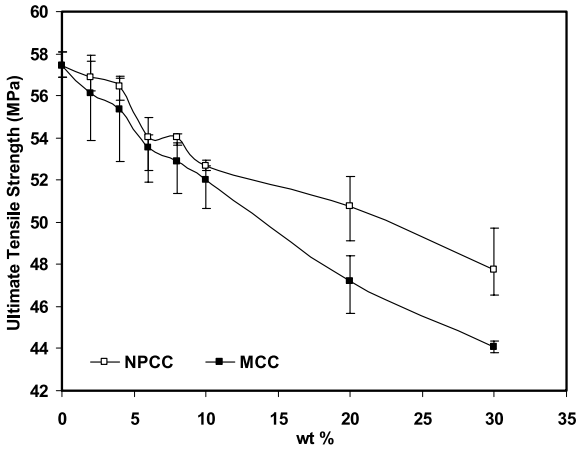

Fig. 4. Tensile strength of NPCC/ABS and MCC/ABS composites with different powder contents.

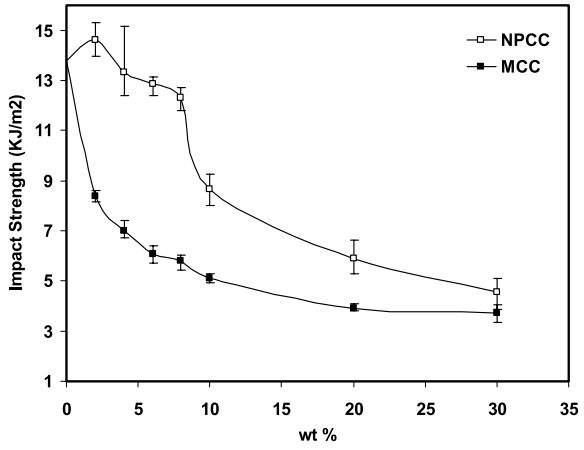

Fig. 5. Impact strength of NPCC/ABS and MCC/ABS composites as a function of powder loading.

a higher tensile strength than its counterpart, especially at high filler ratios (Fig. 4). At low filler ratios, the differences were small. As explained in the last paragraph, the modulus of NPCC/ABS is smaller than that of MCC/ABS due to the small strain when the modulus was calculated. With increasing strain, the stress increased to the threshold of the particle/polymer bonding strength. At this stage, a larger interfacial area meant higher load the specimen could withstand. Therefore NPCC/ABS, with larger interfacial area, had higher ultimate tensile strength than MCC/ABS.

The difference in impact strength between the two composites was much more significant, see Fig. 5. NPCC/ABS had much higher impact strength than its micron-sized counterpart over most of the wt% range. At small filler contents ($\leq$8 wt%), the impact strength of ABS was basically maintained or even slightly improved by the addition of NPCC, whilst the modulus increased by 49% at the same time. This shows the great advantage of using NPCC as strengthening fillers in polymer processing. The first reason for higher tensile and impact strength of NPCC/ABS composites is that NPCC had larger surface area and so larger interfacial area with the polymer matrix. As such, the overall bonding strength between the particle and matrix was higher. Thus, it is to be expected that the composites could stand higher loading under external forces. Secondly, it is well accepted that cavitation and cavitation-induced shear yielding is the dominant mechanism of the toughening of particulate filled polymers [25–30]. Cavitation at the boundary of the particle and polymer phases could trigger a plane-strain to plane-stress transition, leading to shear yielding in the ligament between the two cavities. To make this happen, the surface to surface inter-particle distance (ligament thickness) must be smaller than a critical value. As a reference, the critical thicknesses are found to be 0.30 μm for Nylon/rubber blends and 0.27 μm for SiO2/PP composites, respectively [26,30]. However, in current study, the inter-particle distances in MCC/ABS composites shown by Fig. 1 are much larger than the critical values. Therefore, particulate toughening was unlikely to happen in these composites. In contrast, at the same particle loading, the number density of NPCC particles in the composites was much higher than that of MCC, and the inter-particle distances should be much smaller in NPCC/ABS than in MCC/ABS. The inter-particle distance could decrease below that of the critical ligament thickness value and therefore the possibility of the toughening effect taking place. However, with increasing NPCC loading, particle agglomeration intensified and the inter-particle distance became bigger. This might lead to a decrease in impact strength when the distance was larger than the threshold value (Fig. 5).

3.3. Rheological

G' and G'' of NPCC/ABS and MCC/ABS composites at different powder contents are compared in Fig. 6(a)–(e). For both NPCC/ABS and MCC/ABS, G' and G'' increased monotonically with filler loading, as expected for the filler effect. The characteristic terminal behavior of a homopolymer with narrow molecular weight distribution, i.e. $G' \propto \omega^2$ and $G'' \propto \omega$ was not followed by neat ABS, especially for G'. The frequency dependences were $\omega^{1.3}$ and $\omega^{0.95}$ for G' and G'', respectively. This is understandable since ABS is a tri-block copolymer and its molecular weight distribution is likely to be wide as a mass produced product. In most cases, the shapes of G' and G'' curves of MCC/ABS (Fig. 6(a) and (b)) remained unchanged at different filler contents. The slopes of G' and G'' curves remained the same as neat ABS, i.e. 1.3 and 0.95, respectively. This indicates that the addition of MCC did not notably change the microstructures of the composites and so their rheological natures.

At the same filler contents, NPCC/ABS and MCC/ABS almost had the same G'' values (Fig. 6(b) and (d)), which gave no indication about their structure difference. In contrast, G' is very sensitive to microstructure of materials and is a vital parameter in the study of polymer blends, emulsions and suspensions etc. through rheological tests. Subtle changes in G' can reveal important structural information of the materials. In Fig. 6(c), the frequency dependence decreases monotonically from $\omega^{1.3}$ for neat ABS to $\omega^{0.6}$ for NPCC(30%)/ABS. Plateaus emerge on the curves of 20 and 30 wt% NPCC at low frequencies. This behavior was also observed in triblock copolymers in the ordered state and was attributed to the quasi-tethering of the unlike polymer segments in their respective microdomains [31,32]. Some conventionally filled polymer systems also showed this response when there were strong interactions between the polymer and the filler [33]. The presence of yield phenomena in these systems was identified as the reason. We tend to believe that this typical pseudo-solid-like behavior indicated that a certain NPCC network structure was formed in NPCC/ABS composites [34,35]. This structure was absent in MCC/ABS composites as their G'

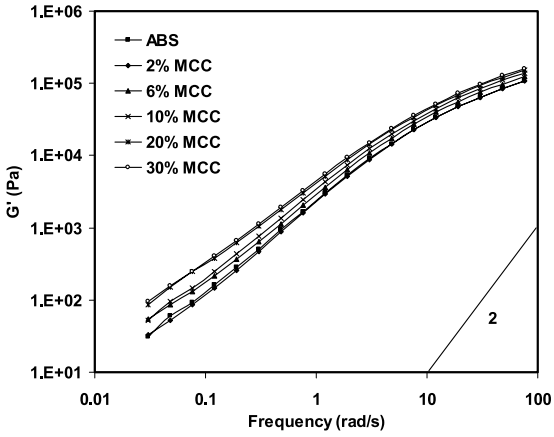

(a) G' of MCC/ABS

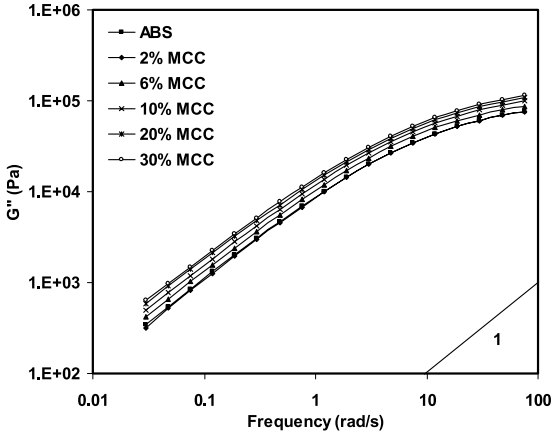

(b) G'' of MCC/ABS

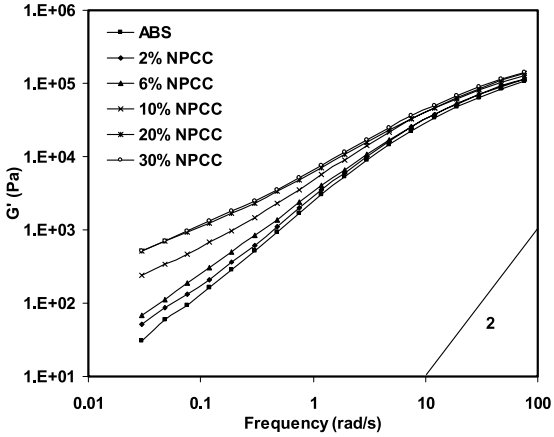

(c) G' of NPCC/ABS

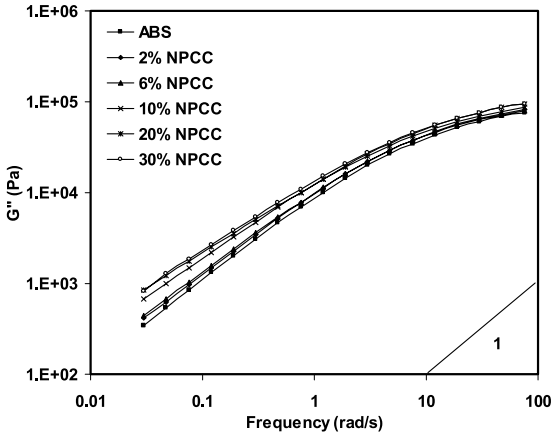

(d) G'' of NPCC/ABS

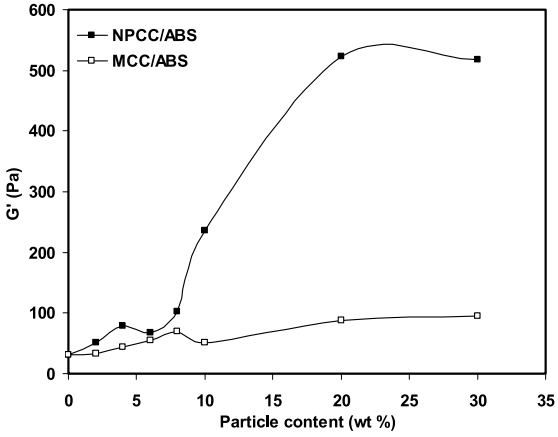

(e) Comparison of G' of NPCC/ABS and MCC/ABS at different particle contents (Frequency: 0.03 rad/s).

Fig. 6. G' and G'' of NPCC/ABS and MCC/ABS composites.

curves show typical patterns of neat ABS melts. Fig. 6(e) reveals the vast difference of G' between NPCC/ABS and MCC/ABS, especially when the particle content is larger than 8 wt%. At the same weight content, the number density of NPCC particles in the composites was much higher than that of MCC, and inter-particle interaction became stronger in NPCC/ABS than in MCC/ABS due to reduced inter-particle distance. This may promote the formation of the

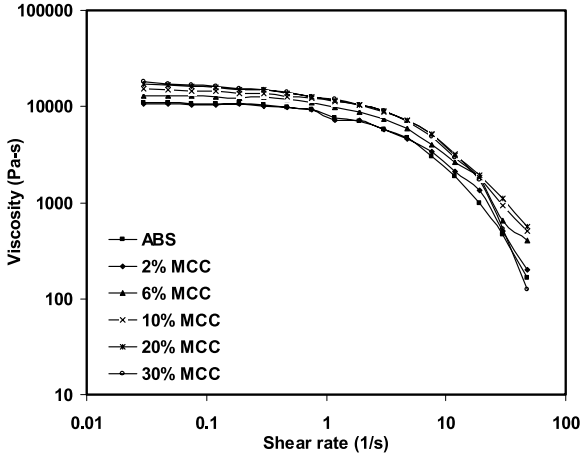

Fig. 7. Viscosity as a function of shear rate of MCC/ABS composites at different MCC contents.

NPCC network structure in the composites during the rheological tests.

The existence of the network structure was further proved by steady shear tests. Fig. 7 shows shear viscosities of MCC/ABS at different MCC contents. Pure ABS shows a Newtonian region when the shear rate is below 1 s^{-1}. Resembling G' and G'' behaviors in Fig. 6(a) and (b), the steady shear viscosity increased monotonically with MCC loading with little change in curve shapes. This again indicated that the addition of MCC just simply increased flow resistance of the polymer matrix without changing its nature.

However, for NPCC/ABS as shown in Fig. 8, the Newtonian region completely disappeared when NPCC content was equal to or above 6 wt%. Shear viscosities decreased over the whole shear rate rage. When shear rate was above 1 s^{-1}, all curves of NPCC/ABS had the same shape of the pure ABS. This implies that the viscosity drop over 1 s^{-1} was due to the molecular orientation of the ABS matrix. Below 1 s^{-1}, pure ABS and NPCC(2%)/ABS had

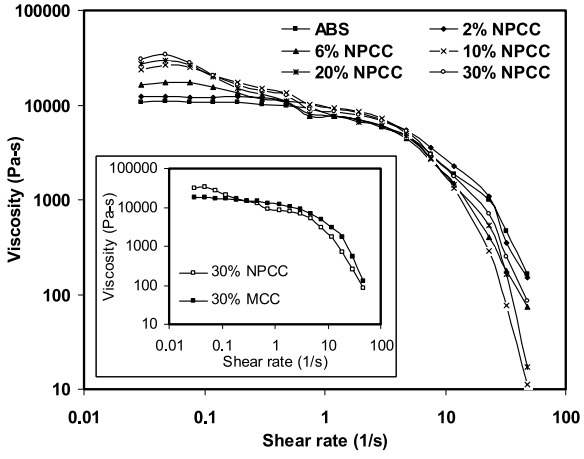

Fig. 8. Viscosity as a function of shear rate of NPCC/ABS composites at different NPCC contents.

constant viscosities while the other composites with high NPCC contents demonstrated early shear thinning behavior. This is ascribed to the continuous orientation or disruption of the NPCC network structure under the shear stress to reduce flow resistance. The insert in Fig. 8 clearly shows the different viscosity behavior between 30 wt% NPCC/ABS and MCC/ABS.

When an ordered structure is forced to flow, a yield stress can often be observed. Above this stress, the structure reorganizes itself along the force direction and flow starts. The viscosity increases at the start of the curves of 6, 20, and 30 wt% NPCC/ABS are of no experimental artifacts. These increases were indications of yield behavior of the network structure. The rheometer employed in this test was shear strain controlled. The motor rotated the bottom plate of the parallel plate fixture at the designated shear rates. The bottom plate then deformed the sample loaded between the bottom and top plate, and a torque was therefore induced. This induced torque was measured by a sensor connected to the top plate of the fixture. In the current test, the motor starts turning the sample at a shear rate of 0.03 s^{-1}. However, the sample did not flow until the yield point was reached (small elastic deformation of the sample takes place before the yield point). The shear stress built up during the course until it reached the yield stress of the sample and caused the sample to flow. Therefore, on the shear stress–shear rate curve, the slopes before and after the yield point originated from different rheological nature. Before the point, the slope was a combined effect of the elastic modulus of the sample and the property (spring factor) of the torque measuring spring of the rheometer. After the yield point the sample started flowing and the curve gave true rheological property of the sample. The slope change at the yield point is evident in Fig. 9(a) when the NPCC content was equal or above 6 wt%. In contrast, since there was no network structure in MCC/ABS composites, no such slope change could be observed for MCC/ABS, see Fig. 9(b). The shear stress evolvements with particle contents of NPCC/ABS and MCC/ABS were compared in Fig. 9(c). The much higher shear stress of NPCC/ABS confirmed the existence of the network structure.

4. Conclusion

Micron-sized and nano-sized calcium carbonate particles were melt compounded with ABS, respectively. Aside from some agglomerations, SEM micrographs demonstrated that NPCC particles were distributed in the ABS matrix in much smaller sizes than MCC. MCC increased the modulus of neat ABS but decreased its tensile and impact strengths. NPCC was superior to MCC in that it increased the modulus and maintained the impact strength. NPCC/ABS property superiority was attributed to its larger interfacial area and cavitation toughening. Rheological tests revealed striking microstructure difference between MCC/ABS and

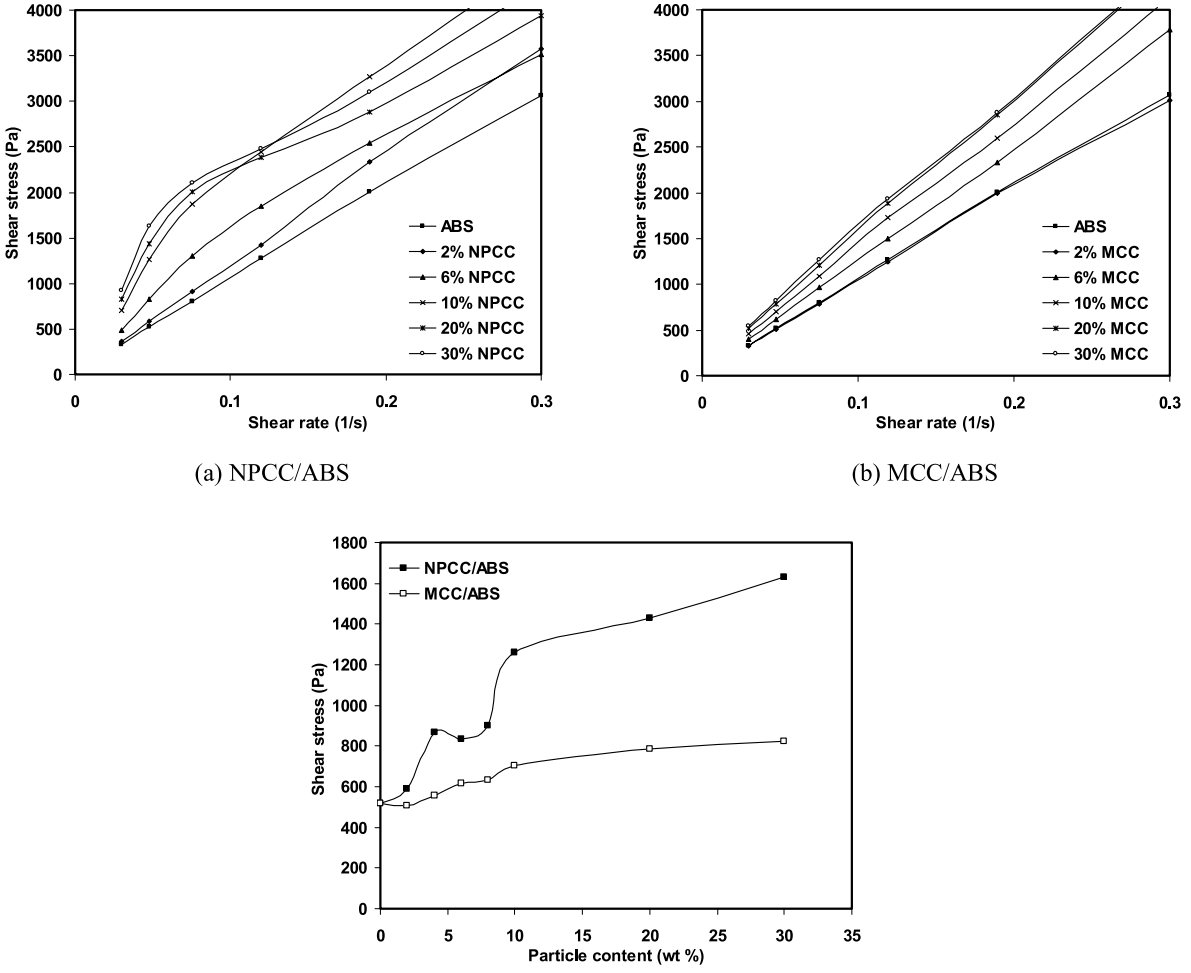

(a) NPCC/ABS

(b) MCC/ABS

(c) Comparison of the shear stresses between NPCC/ABS and MCC/ABS at different particle contents (Shear rate: $0.0475 s^{-1}$).

Fig. 9. Shear stress as functions of shear rate and particle content of NPCC/ABS and MCC/ABS composites.

NPCC/ABS in the molten state. The addition of MCC simply increased the viscosity of the matrix while NPCC changed the rheological response of ABS by forming the ordered structure in the matrix. Loss of Newtonian region, G' plateauing, and yield behavior were among the new rheological phenomena of NPCC/ABS.

References

[1] Sumita M, Shizuma T, Miyasaka K, Ishikawa K. J Macromol Sci Phys 1983;B22:601.
[2] Sumita M, Tsukumo T, Miyasaka K, Ishikawa K. J Mater Sci 1983;18:1758.
[3] Messersmith PB, Giannelis EP. Chem Mater 1994;6:1719.
[4] Messersmith PB, Giannelis EP. J Polym Sci, A: Polym Chem 1995;33:1047.
[5] Yano K, Usuki A, Okada A, Kurauchi T, Kamigaito O. J Polym Sci, Part A: Polym Chem 1993;31:2493.
[6] Lewis TB, Nielsen LE. J Appl Polym Sci 1970;14:1449.
[7] Hasegawa N, Kawasumi M, Kato M, Usuki A, Okada A. J Appl Polym Sci 1998;67:87.
[8] Kojima Y, Usuki A, Kawasumi M, Okada A, Fukushima Y, Kurauchi T, Kamigaito O. J Mater Res 1993;6:1185.
[9] Kojima Y, Usuki A, Kawasumi M, Okada A, Kurauchi T, Kamigaito O. J Polym Sci, Part A: Polym Chem 1993;31:983.
[10] Kojima Y, Usuki A, Kawasumi M, Okada A, Kurauchi T, Kamigaito O. J Polym Sci, Part A: Polym Chem 1993;31:1755.
[11] Lee DC, Jang LW. J Appl Polym Sci 1996;61:1117.
[12] Wang Z, Pinnavaia TJ. Chem Mater 1998;10:3769.
[13] Wang SJ, Long CF, Wang XY, Li Q, Qi ZN. J Appl Polym Sci 1998;69:1557.
[14] Liu LM, Qi ZN, Zhu XG. J Appl Polym Sci 1999;71:1133.
[15] Oriakhi C. Chem Br 1998;34:59.
[16] Rothon R. Particulate-filled polymer composites. New York: Longman; 1995.
[17] Nielsen LE, Landel RF. Mechanical properties of polymers and composites, 2nd ed. New York: Marcel Dekker; 1994.
[18] Di Lorenzo ML, Errico ME, Avella MJ. Mater Sci 2002;37:2351.
[19] Chan CM, Wu JS, Li JX, Cheung YK. Polymer 2002;43:2981.
[20] Li XH, Tjong SC, Meng YZ, Zhu Q. J Polym Sci, Polym Phys 2003;41:1806.
[21] Tang CY, Liang JZ. J Mater Process Tech 2003;138:408.
[22] Liang JZ. Polym Int 2002;51:1473.
[23] Tang CY, Chan LC, Liang JZ. J Reinf Plast Comp 2002;21:1337.
[24] Ray SS, Okamoto M. Prog Polym Sci 2003;28:1539.
[25] Wu S. Polymer 1985;26:1855.

[26] Margonila A, Wu S. Polymer 1988;29:2170.
[27] Pearson RA, Yee AF. J Mater Sci 1989;24:2571.
[28] Wu JS, Yu DM, Mai YW, Yee AF. J Mater Sci 2000;35:307.
[29] Chan CM, Wu JS, Li JX, Cheung YK. Polymer 2002;43:2981.
[30] Rong MZ, Zhang MQ, Zheng YX, Zeng HM, Friedrich K. Polymer 2001;42:3301.
[31] Watanabe H, Kuwahara S, Kotaka T. J Rheol 1984;28:393.
[32] Adams JL, Graessley WW, Register RA. Macromolecules 1994;27:6026.
[33] Agarwal S, Salovey R. Polym Eng Sci 1995;35:1241.
[34] Hoffmann B, Dietrich C, Thomann R, Friedrich C, Mulhaupt R. Macromol Rapid Commun 2000;21:57.
[35] Zhong Y, Wang SQ. J Rheol 2003;47:483.